



# Evaluating elastic wave velocities in Brazilian municipal solid waste

Nataly Aranda<sup>1</sup> · Renato L. Prado<sup>1</sup> · Vagner R. Elis<sup>1</sup> · Miriam Gonçalves Miguel<sup>2</sup> · Otávio C. B. Gandolfo<sup>3</sup> · Bruno Conicelli<sup>4</sup>

Received: 10 December 2018 / Accepted: 20 July 2019 / Published online: 29 July 2019  
© Springer-Verlag GmbH Germany, part of Springer Nature 2019

## Abstract

The sanitary landfills in Brazil are, generally, characterized by their high organic material content (around 60%), presence of different types of mixed wastes, and low compaction energy, which differentiates them from the landfills of developed and high-income countries. To prevent environmental and slope stability risks, it is crucial to understand the behavior of such landfills and the changes in their physical properties over time. The compression wave velocity ( $V_p$ ) and shear wave velocity ( $V_s$ ) are important parameters to subsidize the mechanical characterization of sanitary landfills, using which can be derived the dynamic elastic properties of municipal solid waste (MSW) for stability analysis. Using the geophysical methods of seismic refraction, active and passive multichannel analysis of surface waves, and crosshole test, it was obtained the values of  $V_p$  and  $V_s$  by employing an experimental cell and a lysimeter filled with MSW in the City of Campinas, São Paulo State, Brazil. The results obtained from the crosshole test showed that  $V_p$  ranged from 217 to 252 m/s and  $V_s$  ranged from 86 to 89 m/s. These low values can be attributed to the high content of organic material, low compaction energy, and climatic conditions such as high pluviometry index and high temperatures that together lead to changes in the pore fluid saturation, effective stress, and pore pressure. These values are indicative of the lower limit of the corresponding velocities reported in most literature; however, they are in accordance with the values reported for landfills located in countries with similar socioeconomic and climatic conditions.

**Keywords** Municipal solid waste · Seismic refraction · Multichannel analysis of surface waves · Elastic wave velocities · Crosshole test · Elastic dynamic properties

## Introduction

Landfilling is the main method of municipal solid waste (MSW) disposal, but the waste composition differs from country to country depending on their economic and human development indicators. Countries with low-to-middle income produce more organic waste than countries with high income, which in turn produce more paper waste than the low-income countries (Hoornweg and Bhada-Tata 2012).

In Brazil, the organic waste is approximately 61% of the total waste produced—more than twice the organic waste produced in United States, which is only 25% of total waste (Hoornweg and Bhada-Tata 2012).

The number of sanitary landfills in Brazil has been increasing but despite the established government regulations (ABNT/NB843 1996), there is no guarantee that the laws and processing regulations concerning these landfills have been followed, as seems to indicate the IQR/2017—domestic solid waste quality indicator for 2017 (CETESB 2017) employed by CETESB—Sao Paulo State Environmental Agency for the MSW disposals of Sao Paulo state, the richest and most developed state of Brazil. In addition, the waste types and their respective volumes vary depending on the region of the country. Therefore, it is crucial to understand the behavior of landfills over time to prioritize the use of techniques that prevent the environmental and geotechnical risks caused by poor waste management, such as groundwater contamination and slope instability. The

✉ Nataly Aranda  
aranda.nata@gmail.com

<sup>1</sup> Geophysical Department, Institute of Astronomy, Geophysics and Atmospheric Sciences, University of São Paulo, São Paulo, Brazil

<sup>2</sup> School of Civil Engineering, Architecture and Urbanism, University of Campinas/Unicamp, Campinas, Brazil

<sup>3</sup> Institute for Technological Research - IPT, São Paulo, Brazil

<sup>4</sup> Universidad Regional Amazonica Ikiam, Tena, Ecuador

need for increasing landfill capacity in the most populous regions of the country, owing to the reduction in the number new sites, has led to an increase in the landfill heights, thus requiring a reliable vulnerability assessment of landfill slope failure, which is not a trivial task, considering the rheological properties of such heterogeneous materials.

Owing to the relationship between the elastic properties and the velocities of elastic waves, seismic methods have become a useful tool to subsidize the geotechnical characterization of MSW landfills. Seismic methods such as refraction, crosshole testing, and spectral analysis of surface waves are used to obtain the velocity of the compression wave ( $V_p$ ) and shear wave ( $V_s$ ) as well as the shear modulus ( $G$ ), Poisson's ratio ( $\nu$ ), and Young and bulk moduli ( $E$  and  $K$ , respectively). Properties such as the shear modulus and shear wave velocity are essential for seismic response analysis in areas with high seismicity or those subject to dynamic loads that can cause landslides (Sharma et al. 1990; Choudhury and Savoikar, 2009; Greenwood et al. 2015; Sahadewa et al. 2015). Properties such as Young's modulus and Poisson's ratio are used in static engineering analyses to quantify the response of a material to a change in stress (Kavazanjian 2003; Dixon et al. 2005; Matasovic et al. 2011). The employment of seismic methods to subsidize the evaluation of the mechanical properties of MSW landfills overcomes the limitations of conventional laboratory tests regarding the lack of representativeness of the samples due to the significant spatial variation of materials usually observed in the landfills.

The generally large volume of organic matter from landfills in Brazil, when degraded, generates a considerable volume of gases and fluids (aggravated by the climatic conditions such as high rainfall and high temperatures), which play a key role in the stability of the landfills. In addition, in situ and laboratory tests for evaluation of shear strength and compressibility are not commonly employed in Brazil. The scarce data of the P and S wave velocities for MSW in subtropical climate areas in developing countries like Brazil inspired this study. The elastic parameters when looking for the mechanical characterization of sanitary landfills are very important, but they are poorly studied in regions characterized by high organic content, poor compaction, and climatic humid conditions. In addition, in this study different seismic methods were employed in the same site, rarely recorded in the technical literature, which allows complementary information provided by P and S wave velocity fields and a comparative evaluation of their results with respect to the uncertainties and behaviors of different types of waves (body and surface waves).

We provided and discussed the results obtained by the seismic methods: refraction, crosshole, and multichannel analysis of surface waves employing active and passive sources. The tests were carried out in an experimental cell

built on the Delta A sanitary landfill located in the city of Campinas, state of São Paulo in Brazil. Furthermore, the results of a direct transmission testing performed in a lysimeter filled with the waste disposed on the Delta A landfill were also discussed. Finally, the mechanical properties of the Brazilian MSW were presented considering the velocities of the P and S waves, which presented remarkably low values.

## Review of $V_p$ and $V_s$ geophysical measurements in MSW

Different non-intrusive seismic methods have been used to image and characterize sanitary landfills, including the spectral analysis of surface waves (SASW) (Kavazanjian et al. 1996; Zekkos et al. 2013), MASW (Abreu et al. 2016; Carpenter et al. 2013; Zekkos 2014; Konstantaki et al. 2014; Gaël et al. 2017), and seismic refraction tomography (SRT) (Doll et al. 2001; Wongpornchai et al. 2009). The intrusive seismic methods, which are not commonly used, include downhole (Carvalho 1999; Houston et al. 1995; Sharma et al. 1990) and crosshole (Carvalho 1999; Abreu et al. 2016; Sahadewa et al. 2015) tests.

The compression wave (P-wave) and shear wave (S-wave) velocities for MSW can vary from landfill to landfill owing to several factors. The composition and size of the waste, compaction energy, confining stress, unit weight, and the time under confinement considerably influence the wave velocities in the MSW (Zekkos et al. 2014). The weather conditions also influence the parameters related to the amount of water infiltration in the landfill. The water stored in the waste mass affects the pore-fluid saturation (and thereby, the effective stress, pore pressure, and density) and consequently, it can affect the seismic wave velocities as well as the slope stability.

For regions with temperate or arid climates in the Northern Hemisphere, there are some propositions of a reference shear wave velocity profile when site-specific data are unavailable (Kavazanjian et al. 1996), or empiric and semi-empirical models that can be used to estimate the  $V_s$  of MSW (Zekkos et al. 2014). On the other hand, for landfills located in regions with a humid climate or wet areas and with high organic content (developing countries), there is not sufficient available data to use as a reference (Abreu et al. 2016). Some examples of studies focused on the humid regions in Brazil are those by Carvalho (1999) and Abreu et al. (2016); a representative study for Thailand is by Wongpornchai et al. (2009). Some P- and S-wave velocities for MSW obtained with different geophysical methods around the world are summarized in Table 1. It is important to mention that most of these velocity values are derived from the inversion

**Table 1** P-wave and S-wave velocities measured in different solid waste landfills

References	Local	Method	Depth (m)	$V_p$ (m/s)	$V_s$ (m/s)
Sharma et al. (1990)	Richmond, California	Downhole	0–15.3	716.8 (mean value)	198.3
Houston et al. (1995)	Northwest Regional Landfill Facility, Arizona-USA	Downhole	1.52–6.10	235–300	124–184
Kavazanjian et al. (1996)	Azuza Landfill, California-USA	SASW	0–30	Data unavailable	80–300
Carvalho (1999)	Bandeirantes Landfill, São Paulo, Brazil	Downhole and Crosshole	0–28	190–400	92–208
Doll et al. (2001)	Camp Roberts, California, USA	Seismic Refraction	0–13	761 (mean value)	Data unavailable
Wongpornchai et al. (2009)	Mae-Hia Landfill Sites, Mueng District, Chiang Mai	Seismic Refraction Tomography	0–9	124–849	Data unavailable
Carpenter et al. (2013)	Veolia ES Orchard Hills (Rockford, Illinois)	MASW and Seismic Refraction	0–5	380–460	150–170
Castelli and Maugeri (2014)	Cozzo Vuturo landfill (Sicily, Italy)	Seismic Dilatometer (SDMT)	0–16	Data unavailable	50–400
Zekkos et al. (2014)	Oakland Heights, Michigan, USA	MASW and MAM	0–21	Data unavailable	100–150
	Arbor Hills, Michigan, USA	MASW and MAM	0–19	Data unavailable	100–170
	Sauk Trail Hills, Michigan, USA	MASW and MAM	0–30	Data unavailable	90–160
	Carleton Farms, Michigan, USA	MASW and MAM	0–31	Data unavailable	70–210
Konstantaki et al. (2014)	Wieringermeer landfill, Netherlands	MASW, Seismic Reflection	2–5 5–15	Data unavailable	90–105 132–290
Abreu et al. (2016)	São Carlos Landfill, São Paulo, Brazil	Crosshole and MASW	9–23 0–20	600–1719 197–451	Data unavailable 92–214
Anbazhagan et al. (2016)	Mavallipura Landfill, Bangalore, India	MASW	0–20	Data unavailable	57–125
Gaël et al. (2017)	Mont-Saint-Guibert Belgium	MASW	0–16	Data unavailable	100–180

of seismic data (SASW, MASW, tomography); therefore, the uncertainties related to the non-uniqueness of ill-posed and nonlinear inverse problems must be considered. The inversion processes can be biased, eventually, by wrong choices on the model parameterization, by the used method for data prediction or by the formulation of the inverse problem. Considering this fact and the few data available for the  $V_p$  and  $V_s$  of solid waste in tropical developing countries, it can be concluded that for such countries, the velocities tend to exhibit lower values than those reported for landfills in high-income countries.

## Study sites

The characterization of elastic wave velocities of MSW using different seismic methods was carried out in an experimental cell and a lysimeter, which simulated the cell's conditions. The experimental cell with dimensions of  $80 \text{ m} \times 70 \text{ m} \times 5 \text{ m}$  was filled with MSW and built on top of the sanitary landfill Delta A (Fig. 1) in the city of Campinas, São Paulo in Brazil. The lysimeter had an internal square section of  $1.42 \text{ m} \times 1.43 \text{ m}$  filled with MSW and built in a research area at the University of Campinas—Unicamp (Fig. 2). The city of Campinas lies in a transition region between the tropical climates to the north and subtropical

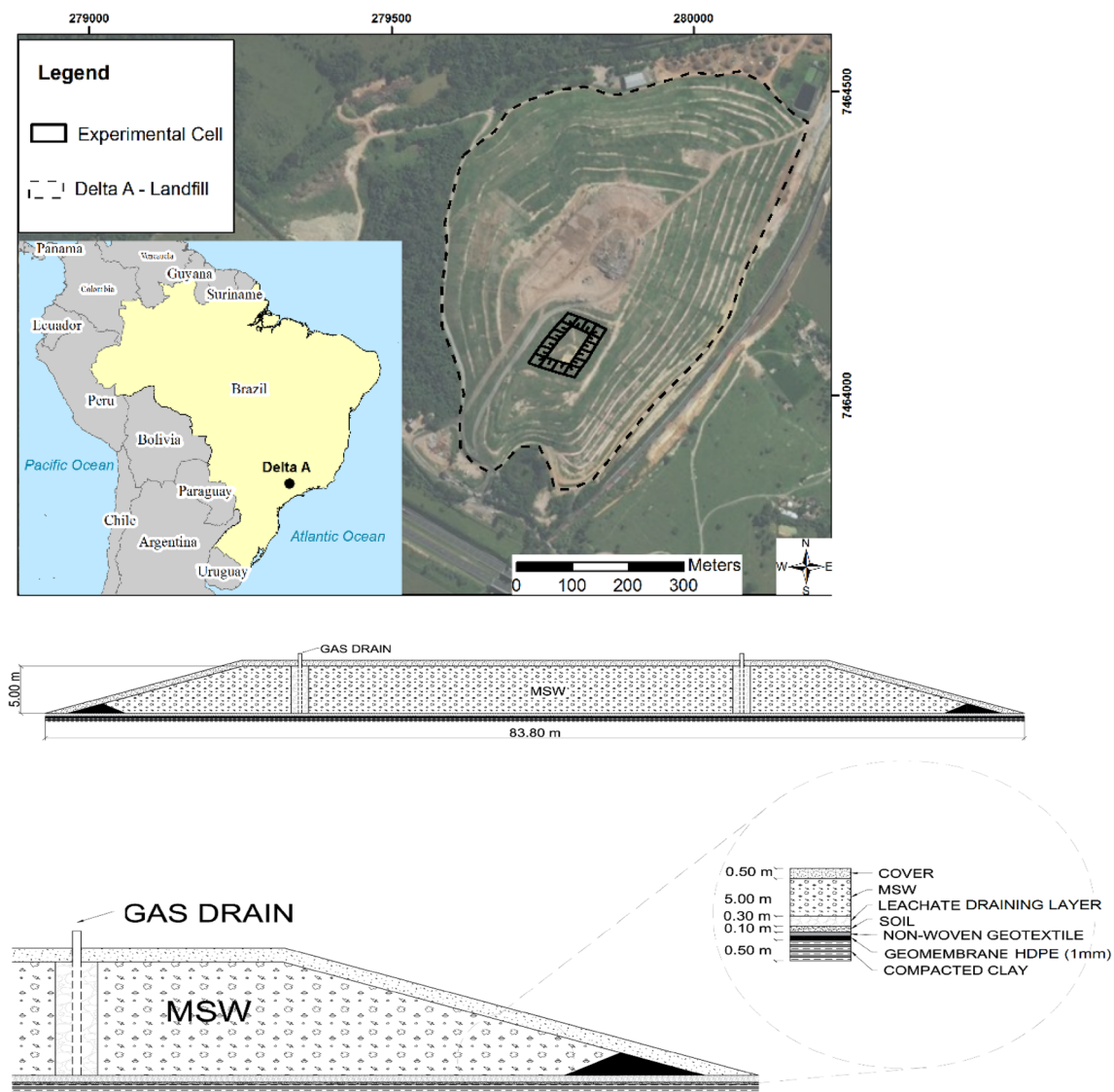


**Fig. 1** Up: Experimental cell (landfill) location on the Delta A Landfill in Campinas-SP in Brazil (UTM coordinates—Zone 23S/WGS84). Down: Cut and detail of the greater diagonal of the experimental cell (Moretto et al. 2017)

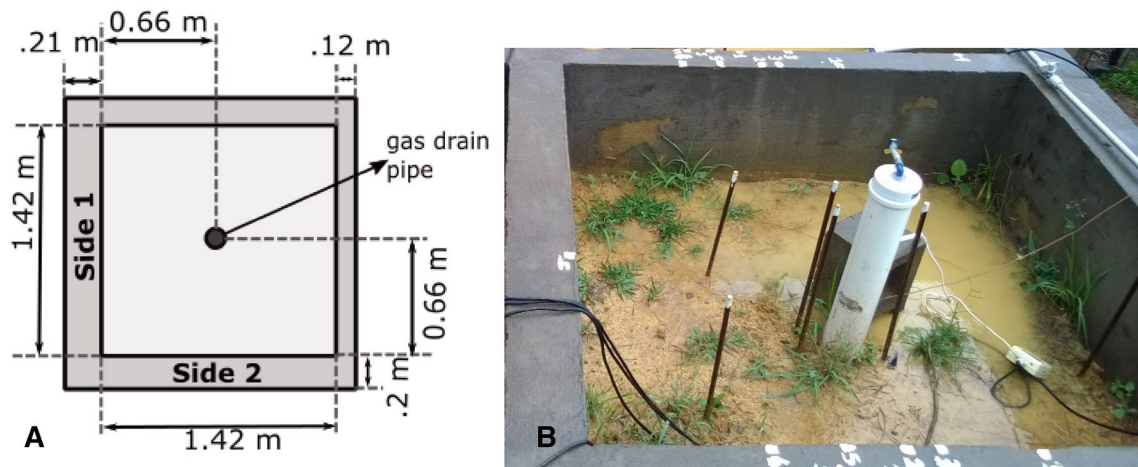


**Fig. 2** a Dimensions of the lysimeter (Favery et al. 2016); top view. b Top view of the lysimeter

climates to the south, with many sources classifying it as having a humid subtropical climate or classified as tropical of altitude (Cwa), with a yearly average precipitation of 1350 mm and an average temperature of 20.7 °C.

### Experimental cell

The experimental cell occupies an area of 5080 m<sup>2</sup> and has a total volumetric capacity for MSW disposal of approximately 15,000 m<sup>3</sup>. Prevailing concepts of landfill engineering were used to construct the experimental cell as follows: a base system composed of 60 cm-thick compacted clayey–sandy silt layer (liner), followed by a 1.5-mm HDPE geomembrane and a nonwoven geotextile (300 g/m<sup>2</sup>); a leachate drainage system formed by a 30 cm-thick layer with stone and a 1.0 m-wide and 30 cm-deep drainage channel located at the base of the cell, diagonally, with a slope of 1.5%; a 5.0 m-thick compacted MSW layer with a gas drainage system constructed with five vertical section drainage tubes having a diameter of 1.5 m; and a 50 cm-thick layer of soil cover composed of clayey–sandy silt. Further details on the construction of the experimental cell can be seen in Benatti et al. (2013).

The experimental cell was designed to receive the MSW generated from the city of Campinas and classified as Class II-A and II-B waste, according to the NBR 10004 (ABNT 2004), which includes non-hazardous inert and non-inert wastes. The waste composition of the cell is as follows: approximately 47.3% organic materials (organic matter and pruning), 12.9% paper (paper and cardboard clean), 13% plastics (hard and soft plastics), 1.2% metals, 1.9% glass, 1.9% debris, 0.9% wood, 5.3% diapers and sanitary pads, and 15.6% other materials (miscellaneous, fabric, Tetra Pak® and toilet waste) (Miguel et al. 2016).

At the time of this research, the experimental cell MSW was already confined 6 years ago. Paixao Filho and Miguel (2017) analyzed the physical and chemical variables of leachate generated by MSW confined in the experimental cell and concluded that MSW was in the phase of methanogenic anaerobic biodegradation.

The Delta A sanitary landfill is in an area geologically made up of rocks of the Itararé Subgroup whose characteristic lithologic strata are mudstones with rhythmic intercalations of sandstones in the lower portion and siltstones in the upper portion. The landfill is located in a humid subtropical climate area, characterized by, generally, dry and mild winters and rainy summers with warm to hot temperatures. The rainiest month is January and the driest month is August. On-site precipitation varies from 200 mm/month in the rainy season (November–March) to 50 mm/month in the driest period (April–September).

### Lysimeter

The lysimeter was filled with the same MSW that was disposed in the experimental cell. It was built using the same steps and features used in the construction of sanitary landfills (a base system by reinforced concrete slab, a leachate drainage system, a gas drainage system, a compacted MSW layer, and a cover system) (Favery et al. 2016). The characterization of the MSW that filled the lysimeter are as follows: 53% organic, 14.6% paper, 12.5% plastic, 1.9% metal, 1.8% glass, 1.1% inert, and 14.6% other (Favery et al. 2016). The cover layer is composed of compacted soil and crushed stone (gravel). Figure 2 shows the lysimeter dimensions. The characteristics for the lysimeter are presented in Table 2. At the date of this research, the MSW confined in lysimeter was 3 years old.

**Table 2** Characteristics of the lysimeter after it is filled, adapted from Favery et al. (2016)

	MSW layer	Cover layer	
		Soil	Gravel
Weight (kg)	2247.4	532.9	1714.0
Unit weight (kN/m <sup>3</sup> )	5.93	17.91	18.25
Final thickness (cm)	156.8*	53.2	

\*Discounted initial height (191.8 cm) of the settlement between 2016 and 2018 (35 cm)

## Methods

The velocities of the seismic waves are determined by the elastic parameters and densities of the materials. Different seismic methods can be used to obtain the values of P- and S-wave velocities, and subsequently, the elastic parameters. In this study, multichannel analysis of surface waves (MASW), seismic refraction tomography, seismic crosshole, and the measurements of directly transmitted waves (similar to crosshole tests) were applied.

In the experimental cell, the seismic data were collected using surface methods by employing three different arrays: L1, L2, and L3 (Fig. 3). A P-wave refraction survey was conducted along profile L1, and MASW surveys were conducted along profiles L2 and L3, using active and passive sources, respectively. The crosshole seismic data were acquired in two borehole sets: CH-1 and CH-2 (Fig. 3). The measurements of direct waves were carried out in the lysimeter.

## Seismic refraction tomography (SRT)

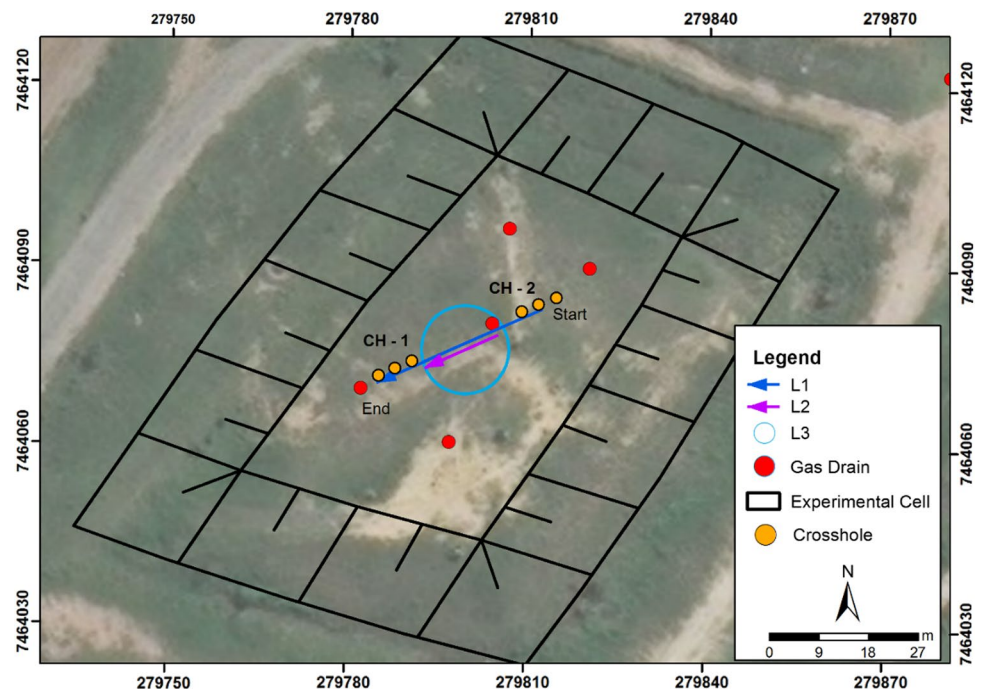
The SRT was applied in the experimental cell to map the near-surface P-wave velocities by inverting the first arrival times.

The arrangement used in the refraction survey consisted of 72 14-Hz vertical geophones, positioned every 30 cm along L1, connected to a 24-bit seismograph. The source was an 8-kg sledgehammer vertically striking a metal plate. Eleven shots were positioned every 1.8 m along the profile.

The data were processed and analyzed using the Rayfract<sup>®</sup> software. This software estimates the velocity model by determining the travel times of the seismic waves by solving the eikonal equation (Schuster and Quintus-Bosz 1993) by finite differences in a process, called Wavepath Eikonal Travel time inversion (WET). An initial smooth velocity model is first obtained from the seismic traveltimes data; then, the software iteratively solves the wave equation to determine the theoretical times and inverts the data using the back-projection formula (Schuster and Quintus-Bosz 1993). The following are the main steps in SRT using Rayfract<sup>®</sup>:

1. Picking the first breaks in the seismograms.
2. Setting the geometry information (position of shots and receivers).
3. Running inversion-smooth WET with one-dimensional (1D)-gradient initial model.
4. Editing the WET and 1D-gradient parameters and settings to improve the obtained velocity model.

**Fig. 3** Experimental cell and acquisition line locations. L1 is the seismic refraction survey line. L2 is the active MASW line, and L3 is the passive MASW line



### Multichannel Analysis of Surface Waves (MASW)

The MASW method was employed to obtain shear wave velocity profiles of the near-surface in the experimental cell. The velocity profiles were obtained using the record of the Rayleigh waves using active and passive sources.

The data processing (Fig. 4), employing the software SurfSeis<sup>®</sup>, consisted of five basic steps:

1. Acquisition of multichannel shot records.
2. Generation of the dispersion images by a two-dimensional wavefield transformation of the field records.
3. Extraction of the fundamental mode of the dispersion curves (one curve per record).
4. Inversion of the dispersion curves to obtain 1D Vs velocity models (depth).

The active MASW survey setup consisted of 48 4.5-Hz vertical geophones positioned every 30 cm along L2 and an 8-kg sledgehammer as seismic source. The shots were given at different distances from the first and the last geophones. The minimum offsets employed were 2 m, 4 m, 6 m, and 8 m. For the passive MASW survey, the arrangement employed a two-dimensional circular layout (L3 in Fig. 3), with the 48 vertical geophones positioned every 1.05 m.

The data processing using SurfSeis<sup>®</sup> included the following: shot records input, geometry assignment, mute filtering of air waves and refracted wave first arrivals, and generation of the phase-velocity dispersion image for each record. After obtaining the individual dispersion images, different dispersion images were stacked to obtain a better dispersion image (higher signal-to-noise ratio and broader spectrum). Finally, the dispersion curves from the final dispersion images were extracted, which were inverted to obtain the shear wave velocity profiles.

For the active method, the dispersion images were obtained from the seismograms recorded using different minimum offsets. The dispersion images obtained for shot

gathers given at longer minimum offsets ( $\pm 6\text{ m} \pm 8\text{ m}$ ) were of better quality than those obtained for shots given at smaller minimum offsets ( $< 6\text{ m}$ ). Next, four dispersion images derived from the shot gathers acquired with minimum offsets of 6 m and 8 m from the beginning and from the end of the array (opposite sides of the array) were stacked.

For the passive MASW method, several acquisitions were made by changing the record length (RL) as follows: 15 s, 20 s, 30 s, 40 s, 50 s, and 60 s. For each of the record lengths, several records were acquired, obtaining in total 73 records. The best dispersion images were obtained for the 60-s RL seismograms. Four dispersion images were stacked, and the dispersion curve was extracted. The dispersion images processed from active and passive data were stacked to enlarge the analyzable frequency range of dispersion (and therefore, depth) and to better identify the modal nature of the dispersion trends (Park et al. 2007).

The dispersion images processed from active and passive data can be stacked to enlarge the analyzable frequency range of dispersion (therefore to enlarge the investigation depth range) (Park et al. 2007). The SurfSeis software allows to combine dispersion images whenever the images are generated with the same criteria, that is, with the same frequency bands and phase velocity. So, the dispersion images, obtained with active and passive source, were generated using maximum frequency of 50 and maximum phase velocity of 500 m/s. Shear wave velocity measurements at the surface were obtained by combining the active and passive MASW method.

### Crosshole seismic test

The crosshole seismic test was employed to measure the velocity of the seismic waves between the adjacent boreholes at different depths. Usually, at least two boreholes are needed: one to place the P- or S-wave source and another to place a 3C-geophone (one vertical and two horizontal components) that registers the waves propagated

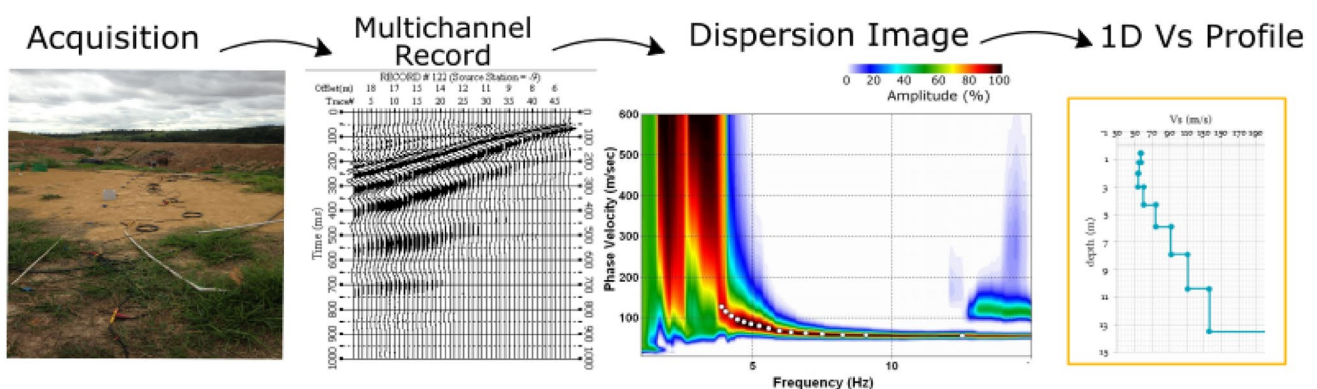


Fig. 4 MASW analysis procedures

directly between the source and receiver. The source and geophones are placed at the same depth level for each record.

The data were acquired in two boreholes sets, each one with three boreholes positioned every 3 m. The P and S energy sources were placed in the middle borehole, and the waves were recorded by the 3C-geophones placed in the two end-boreholes. The maximum depth of the boreholes was 2.5 m to avoid any damage to the bottom liner, geomembrane, and geotextile of the experimental cell. Data were acquired every 0.25 m, starting at 0.75 m and ending at 1.75 m, to allow the free operation of the S-wave source. For each set of boreholes, two separate tests were performed. First, a P-wave generating source, which was a cylinder camera that burst a PVC membrane through the injection of CO<sub>2</sub> was employed. Next, it was employed the S-wave generating source, which was a sliding piston which hit (downward and upward) a metal cylinder clamped at the borehole wall. This reverse polarity seismic source helps identify the S-wave arrival. The same 3C-geophones were employed for both tests.

The data were analyzed using the Seismic Unix software (Cohen and Stockwell 1996) for picking the P- and S-wave arrivals. The P-wave velocities were obtained using the first deflection criteria to pick the first arrivals on the signals recorded by the two horizontal-component receivers. The S-wave velocity was obtained using the criteria of the polarity inversion between the upward and downward blow on the signal recorded by the vertical-component receiver.

### Direct wave test

The measurements of directly transmitted waves were done in the lysimeter. The waves were generated at the walls of the lysimeter (Sides 1 and 2 of Fig. 2) when they were impacted with a small sledgehammer. The waves were recorded by a 3C-geophone located in the central gas drain pipe (Figs. 2 and 5). The data were acquired every 20 cm, starting at the depth of 0.08 m. The data were obtained by shooting on Sides 1 and 2, before and after the lysimeter was drained. The horizontal distance between the shots and the geophone, which was measured at the surface, was 0.7 m, as indicated in Fig. 5.

The P-wave velocities were obtained after picking the first arrivals on all the signals recorded by the two horizontal-component receivers. The data were acquired from the lysimeter, shooting on two sides: side 1 and side 2 (Fig. 2). First, the data were collected by shooting on side 1; then the lysimeter was drained (9 L of leachate) to the field capacity, and finally the data were collected by shooting on side 2.

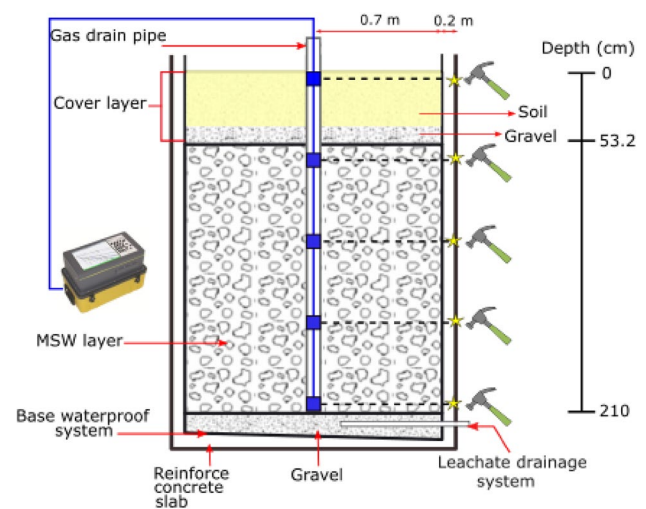


**Fig. 5** Schematic of the modified direct wave test in lysimeter. MSW thickness 191.8 cm, cover layer thickness 53.2 cm

## Results

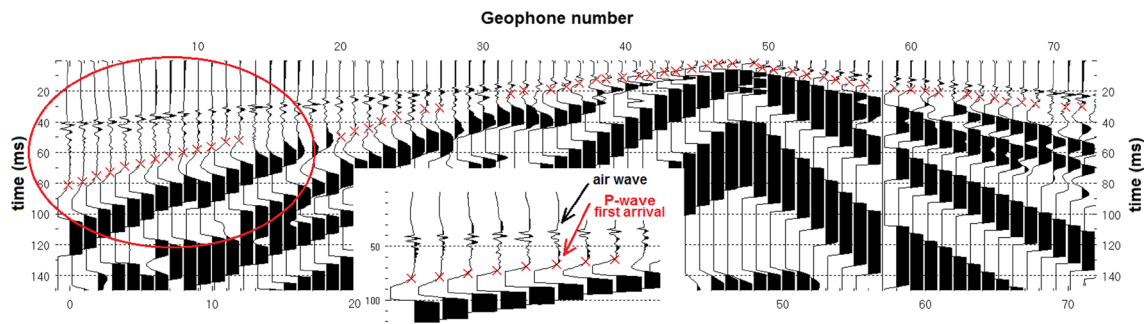
### Seismic refraction tomography

Figure 6 shows an example of the seismogram and the first breaks picked. It can be clearly seen that the P-waves arrive after the air waves.

The P-wave velocity model and the respective wave path coverage plot are shown in Fig. 7. The velocity model shows very low velocities; however, the velocity gradient assumptions of the tomography methods require that the retrieved values of  $V_p$  should be considered with caution if the gradient is not uniform along the profile (Sheehan et al. 2005). The increasing  $V_p$  from ENE to WSW, shown in the tomography image of Fig. 7a, should also be interpreted with caution at the ends of the profile as the density of rays is low (Fig. 7b); this affects the inversion result. In the high-density region of the coverage plot, approximately between 5 and 17 m (Fig. 7), the P-wave velocities ranged between 160 and 220 m/s.

The low P-wave velocities obtained with seismic refraction are in accordance with the results obtained for the upper stratum by Carvalho (1999), Zalachoris (2010), and Abreu et al. (2016), although the velocities obtained in the present study are even lower. Carvalho (1999) obtained the  $V_p$  of 195–400 m/s for the Bandeirantes Landfill in São Paulo, Brazil, using crosshole and downhole tests, and Abreu et al. (2016) obtained the  $V_p$  of 197–316 m/s using the crosshole tests.





**Fig. 6** Example of the seismogram obtained from the seismic refraction survey. The red crosses are the first breaks picked by Rayfract® software. The P-wave arrival times are greater than the time arrival

of the air waves (recognized by their higher frequency and smaller amplitude) as can be noticed by the zoomed traces (identified by the ellipse)

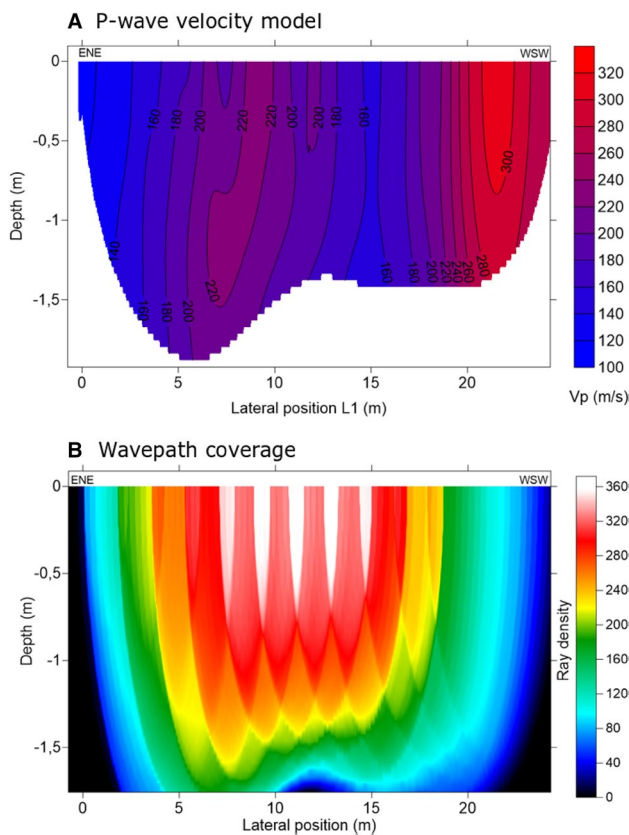


**Fig. 7** a P-wave velocity model retrieved from the seismic refraction analysis (model with 2.9% RMS error) and b the respective wavepath coverage plot

**Multichannel analysis of surface waves (MASW)**

Figure 8 shows the stacked dispersion image of the passive and active MASW images. The combination of the two images has better defined dispersion curves for both low and high frequencies; therefore, the result of the inversion of the dispersion curve provides a more complete profile than the individual analysis of each image.

The Vs profile retrieved from the inversion of the combined dispersion curve is shown in Fig. 9. The results show that up to a depth of 4.3 m, the velocity can be considered constant, with an average of 58 m/s, which is representative of the velocity of the solid waste from the experimental cell. Then, from 4.3 to 5.8 m, the velocity increases to 75 m/s. This increase in velocity can be associated with the compacted soil layer located at the base of the experimental cell. The velocities obtained at greater depths (exceeding 5.8 m) are related to the old waste landfill, on which the experimental cell was built. The average velocity of the first 5 m of the old landfill (from depths of 5 to 10 m) was 84 m/s, and it increased to 135 m/s at a depth of 16 m.

**Crosshole**

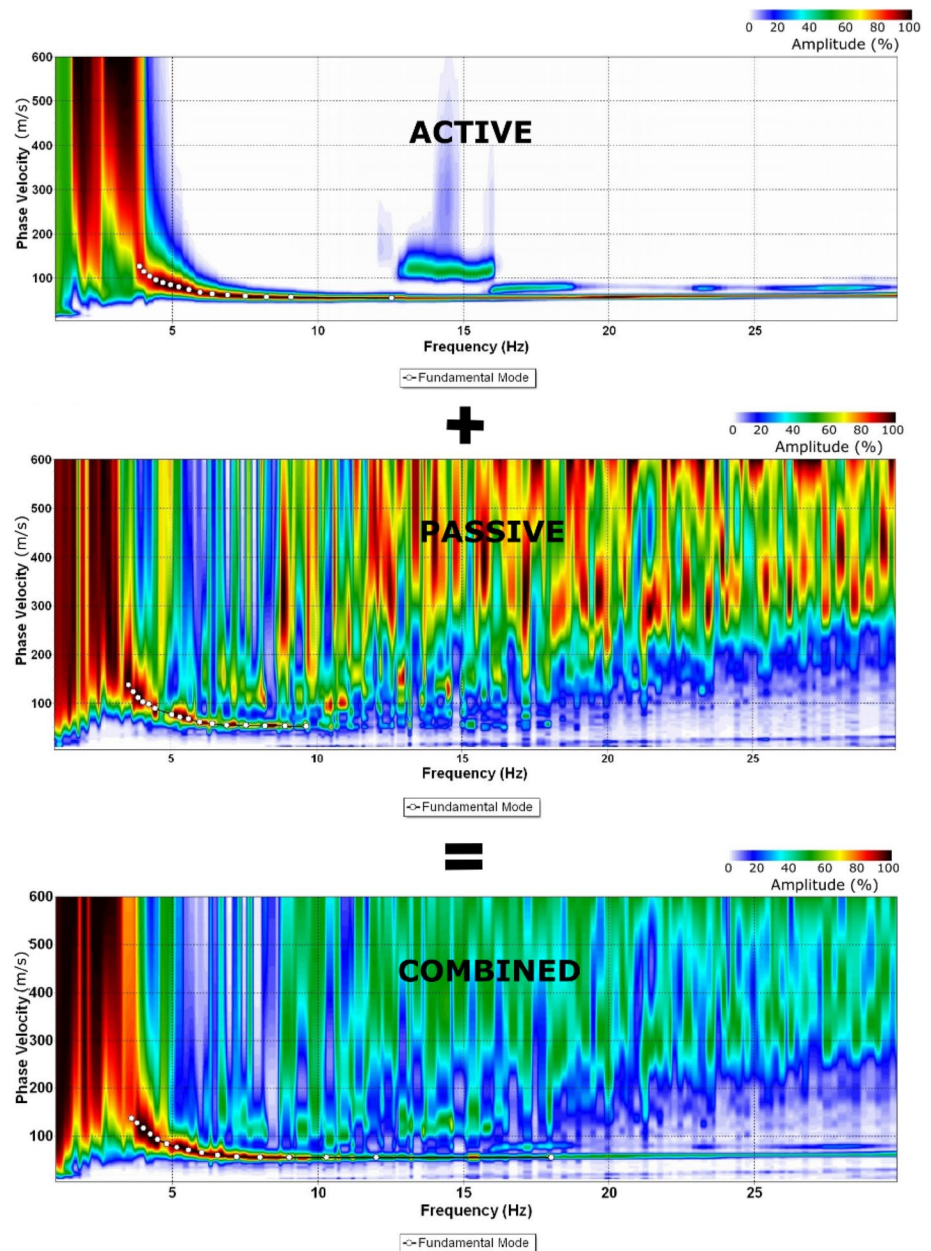
Figure 10 illustrates the seismograms obtained for the CH-2 borehole set at the depth of 1.5 m. It shows two seismograms recorded by the vertical sensor (S-wave reverse polarity source, upward and downward impacts) and the horizontal sensor (P-wave source).

The P- and S-velocities obtained for the two crosshole tests (CH-1 and CH-2) are presented in Fig. 11. For each level, at each crosshole set, two P-wave seismograms and two S-wave seismograms were obtained. Therefore, the velocity profile in Fig. 11 provides the average velocity value for each level and the respective standard errors.

**Direct waves**

Figure 12 shows an example of the obtained seismograms (zoomed image) and the first arrivals that were picked for the MSW layer (1–2 m deep). The seismograms that are shown in black were recorded by shooting at side 1, while the blue ones were recorded by shooting at side 2. It can be seen that there is coherence in the data for the waves obtained for the two sides of the lysimeter at the same depth.

**Fig. 8** Dispersion images and dispersion curves obtained from active MASW, passive MASW, and the combination of both active and passive MASW



The  $V_p$  profiles retrieved from the direct waves are shown in Fig. 13. The P-wave velocity values indicate the average values between the  $V_p$  values obtained from the two horizontal-component seismograms, and the error bars denote the standard error. From Fig. 13 it can be seen that the velocities obtained for the soil layer are lower than the velocities obtained for the upper layer of gravel (250 m/s at a depth of 0.68 m). The high velocities in the MSW observed for depths greater than 2 m can be attributed to the influence of the reinforced concrete base of the lysimeter and the gravel of the leachate drainage base, for which the first arrivals that are picked are related to the path through the wall and base (path of least time) and not the one through the solid

waste layer, which goes directly from the source point to the geophones.

Here, the analysis of the P-wave velocity profile is restricted to depths of 1–1.8 m, that is, only for the first 1 m of the solid waste layer (velocities obtained without the influence of concrete or gravel). Figure 13 also shows a zoomed image of the P-wave velocity profile for the waste layer. The P-wave velocities for the solid waste layer obtained from the records for shooting at side 1 (undrained) and side 2 (drained) do not vary significantly. The 9-L of drained leachate were found in the impermeable base and not in the waste layer; therefore, there was no significant difference in the velocities of the waste layer before and after

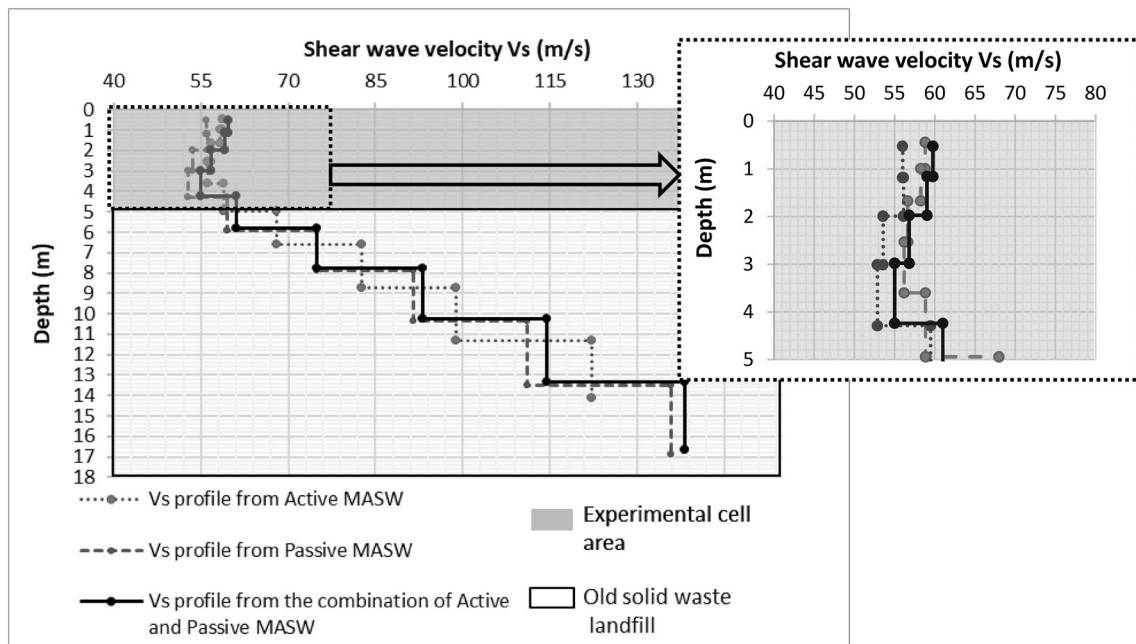


Fig. 9 Shear wave velocity profile obtained from the inversion of the combined passive and active dispersion curves

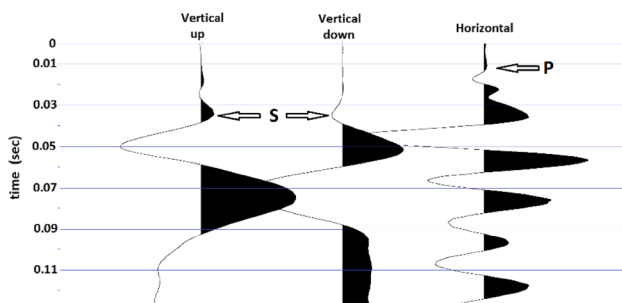


Fig. 10 Typical seismogram of the crosshole test at the depth of 1.5 m

being drained. The average P velocity for the solid waste layer ranged between 185 and 244 m/s, which agreed with the results obtained in the seismic refraction tomography.

### Elastic properties

Using the relationships between the elastic properties and the compressional and shear wave velocities, the elastic parameters for the MSW from Campinas sites were found. First, the unit weight of the MSW was calculated and then the density derived. The dynamic elastic parameters were estimated using the  $V_p$ ,  $V_s$ , and density values.

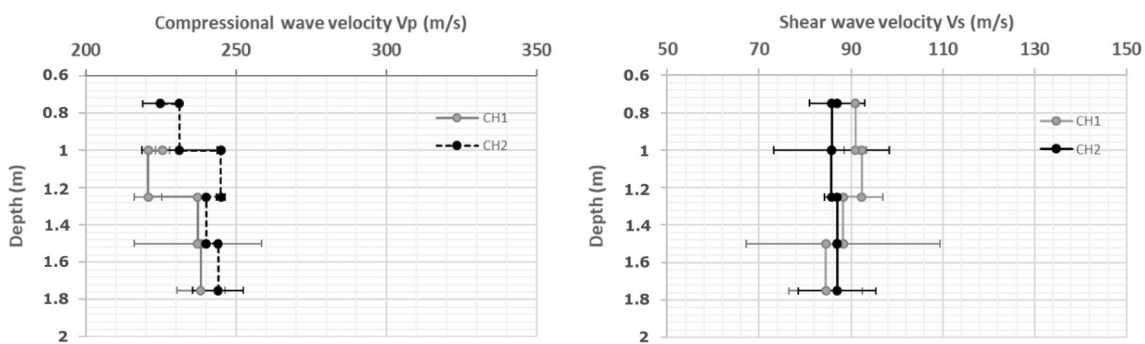
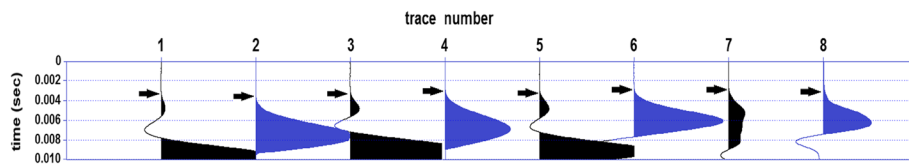
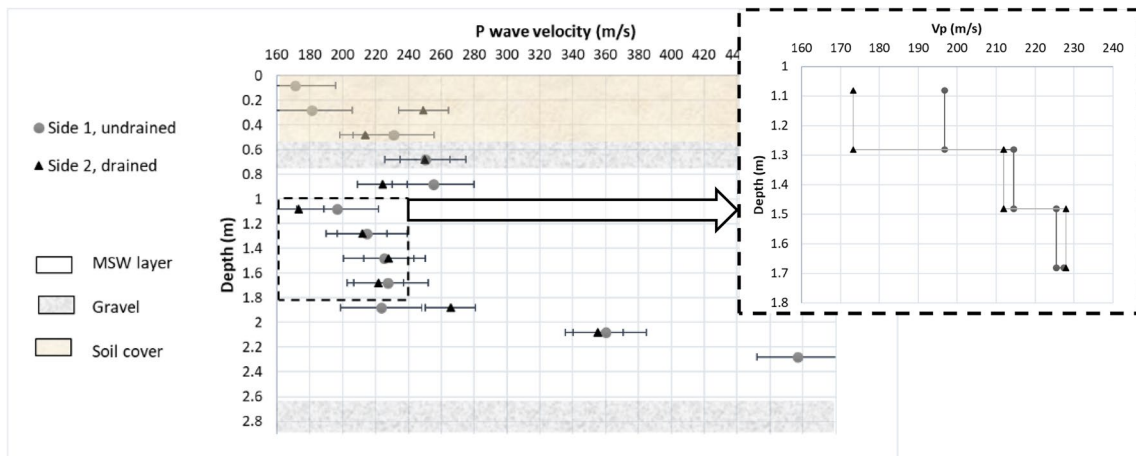


Fig. 11 Compressional and shear wave velocities obtained with crosshole test for the two crosshole tests (CH-1 and CH-2)



**Fig. 12** Seismogram obtained in the waste layer for shots given at side 1 undrained (black waves) and for shots given at side 2 drained (blue waves). Traces 1 and 2 were recorded at a depth of 1.08 m; traces 3 and 4, at a depth of 1.28 m; traces 5 and 6, at a depth of 1.48 m; and traces 7 and 8, at a depth of 1.68 m



**Fig. 13** Velocity profile for the lysimeter from shots in side 1 (triangle) and side 2 after draining the leachate (point). The colorless area represents the solid waste layer, the area in pink represents the soil

layer, and the gray area represents the gravel layer. The zoomed area shows the P-wave velocity profile for the solid waste layer, based on the data obtained by shooting on two sides of the lysimeter

### Unit weight

By employing the empirical relationship between S-wave velocity ( $V_s$ ) and unit weight ( $\gamma_{waste}$ ) proposed by Choudhury and Savoikar (2009) for landfill materials, Eq. (1),

$$V_s = \frac{1}{0.0174 - 0.000978\gamma_{waste}}, \quad (1)$$

an average unit weight of  $6.1 \text{ kN/m}^3$  from the  $V_s$  values was obtained from the crosshole tests. This value agrees well with the value projected for the lysimeter ( $5.93 \text{ kN/m}^3$ ) and is lower than the estimated value for the experimental cell ( $8 \text{ kN/m}^3$ ). Considering that the age of the experimental cell is 6 years, and that its MSW is already in the phase of methanogenic anaerobic biodegradation (Paixao Filho and Miguel 2017), it was expected that the unit weight would increase, since the easily degradable wastes would have already been transformed into leachate and biogas, which were drained of the cell. However, because the experimental cell has not been built with daily layers of compacted soil and yet is not confined laterally or vertically, and is, therefore, not subjected to an increase in vertical stress or impedance of the horizontal displacements, the unit weight value

was low. Nonetheless, this fact should be confirmed through a measurement of the unit weight in the experimental cell, which could not be done to date. However, it can be seen in Fig. 14 that it is in agreement with the values derived by Konstantaki et al. (2016) from MASW (Rayleigh and Love waves) and S-wave seismic reflection data using the same relationship (Fig. 14).

### Dynamic elastic parameters

The evaluation of the elastic parameters in MSW has gained importance because it is a basic step in seismic response analysis, evaluation of slope stability, and the design of MSW landfills. With prior information about the density mass ( $\rho$ ) of the medium and measurements of the compressional wave velocity ( $V_p$ ) and shear wave velocity ( $V_s$ ), it is possible to calculate the elastic parameters such as Young's modulus ( $E$ ), Poisson's ratio ( $\nu$ ), and shear modulus ( $G$ ). Equations (2)–(4) describe the relationships between the elastic wave velocities ( $V_p$  and  $V_s$ ) and the elastic parameters

$$\nu = \frac{(V_p/V_s)^2 - 2}{2(V_p/V_s)^2 - 2} \quad (2)$$

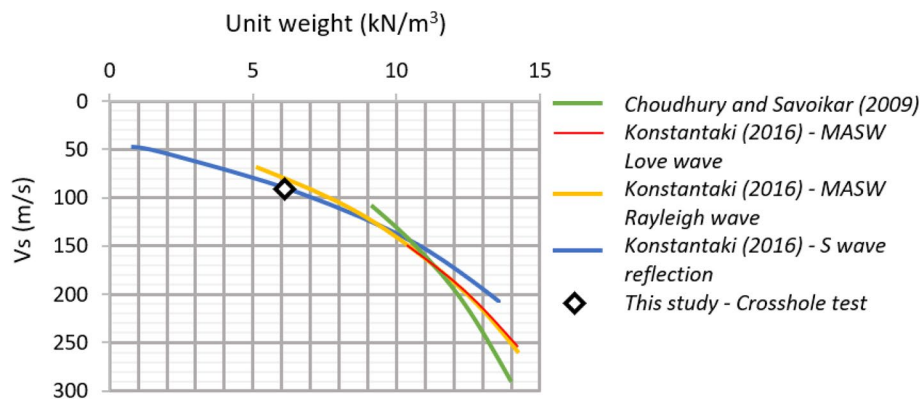


**Fig. 14** The relationship between the unit weight and S-wave velocity from the studies of Choudhury and Savoikar (2009) (compilation of various studies) and Konstantaki et al. (2016) (in Twence landfill in Hengelo, the Netherlands, 30 years of grounding), obtained using

the MASW-Love wave, MASW-Rayleigh wave, and S-wave reflection methods. The diamond mark indicates the value derived from the crosshole data obtained in this study for the experimental cell (6 years of grounding)

$$E = V_p^2 \rho \frac{(1 - 2\nu)(1 + \nu)}{1 - \nu} \tag{3}$$

$$G = \rho V_s^2 \tag{4}$$

With the values of  $V_p$  and  $V_s$  obtained from the crosshole test and a density of  $627 \text{ kg/m}^3$  (obtained from the  $6.1 \text{ kN/m}^3$  unit weight), the elastic parameters for the MSW in the experimental cell was calculated (Table 3).

### Discussion

In this study, it was shown that the P-wave and S-wave velocity values obtained from Brazilian landfills are lower than most of the values reported in the literature (Table 1). Nevertheless, when the comparison is restricted to studies in humid regions and with emerging economies, where the composition of waste and the degree of compaction are supposed to be similar, these results agree.

The  $V_p$  values compiled from the literature for up to a depth of six meters from tropical and subtropical areas and the results of this study are shown in Fig. 15. The P-wave velocities obtained in this study for the experimental cell, by using tomography inversion and crosshole test, are between 160 and 220 m/s for the first 1.6 m depth, considering the results of the seismic tomography in the region with the highest density of rays (Fig. 7). The minimum  $V_p$  values are lower than the corresponding values reported by Carvalho (1999) and Abreu et al. (2016); however, they are within the range of velocities

reported by Wongpornchai et al. (2009) ( $V_p$  of 124 m/s). On the other hand, the  $V_p$  values obtained by the lysimeter agree with the results of Abreu et al. (2016).

Similarly, the shear wave velocities obtained in this study for the experimental cell, by using MASW and crosshole tests, are lower than the velocities reported by other studies (Fig. 15). However, for the old landfill located below the experimental cell, the velocities are in the range of velocities reported by Anbazhagan et al. (2016) and are very close to the lower boundary of the shear wave velocities reported by Abreu et al. (2016) and Carvalho (1999).

It is important to mention that the results obtained in this study with crosshole seismic tests are more accurate than those obtained with MASW or seismic tomography which include inversion processes. This is due to the nature of the crosshole method that records the waves that travel directly from the source to the receivers. Thus, the measured travel times are converted into velocities directly without the employment of inversion methods.

The study by Sahadewa et al. (2011) suggested that the climate is one of the factors that can influence the shear wave propagation that affects the degradation of the waste matter. Their conclusion was based on a comparison of the  $V_s$  values obtained from four landfills in southeast Michigan (75–210 m/s), which has high precipitation (750–1000 mm), with the velocities obtained by Kavazanjian et al. (1996) in south California (125–325 m/s), which has low precipitation (250–380 mm). The southeast Brazilian region has also high rainfall rates (characteristic of subtropical climate) that

**Table 3** Elastic parameters calculated from the values of  $V_s$  and  $V_p$  obtained by the crosshole test and a density of  $627 \text{ kg/m}^3$

Depth	$V_p$ (m/s)	$V_s$ (m/s)	$\gamma$ ( $\text{kN/m}^3$ )	$\nu$	$G$ (MPa)	$E$ (MPa)
0–1.75 m	217–252	86–89	6.1	0.43–0.47	4.6–5.0	6.3–10.9

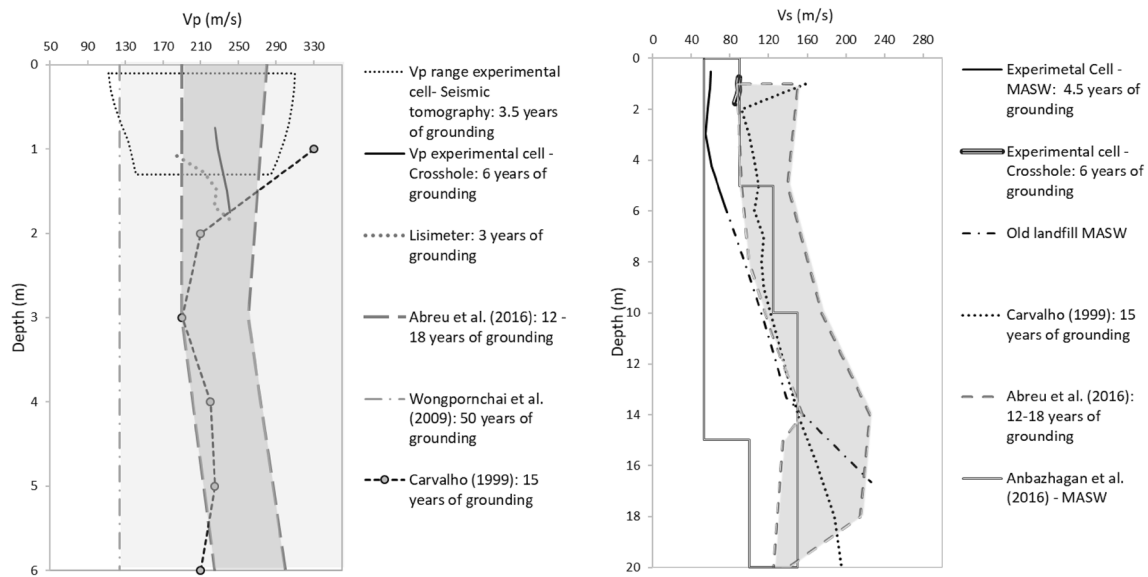


**Fig. 15** P- and S-wave velocities obtained in this research compared to those obtained from other studies in developing countries and humid climate areas. The lower and upper limits for the studies represent the minimum and maximum velocities obtained for each depth

should contribute to the low values of the shear wave velocities observed.

These values reveal peculiar aspects regarding the mechanical characteristics of Brazilian landfills. The current understanding of waste behavior, if valid for the landfills of the northern hemisphere (although the engineering properties can vary due to many factors), is not valid in Brazil. Furthermore, information on the mechanical properties of Brazilian landfills is scarce and sometimes contradictory (Carvalho 1999). The use of laboratory or in situ testing is not a reality. Usually, the mechanical properties related to waste stability are estimated through back analysis of landfill slope failures.

We believe that the low velocity values are due to the presence of gas in the pores, which softens the elastic frame. The high organic matter content (47.3%) provides high moisture content and controls the anaerobic biodegradation process, i.e., the generation of gases and leachate, thus influencing the elastic properties. Paixao Filho and Miguel (2017) reported that MSW confined in experimental cell was in methanogenic phase in which there is the predominance of the methane generation. Moretto et al. (2017) detected some zones of concentration of leachate in MSW mass of the experimental cell; however, most of the MSW mass is not saturated by liquids.

The unit weight of new grounded MSW is between 4.0 and 16.0 kN/m<sup>3</sup>. Low unit weight is characteristic of MSW with low compaction energy and soil content (Zekkos et al. 2006). In this study, the low unit weight, i.e., 6.1 kN/m<sup>3</sup>, was consistent with the MSW subjected to low compaction energy (two or three passes of the Caterpillar D6) and

without the presence of daily layers of compacted soil, as was the case with the experimental cell MSW. This value is also consistent with the unit weight obtained for MSW in São Carlos-Brazil, which ranged between 6 to 9 kN/m<sup>3</sup> for 5 m depth (Abreu 2015).

Through an analysis, Zekkos et al. (2008) showed that the unit weight has some impact on the shear wave velocity and shear modulus, increasing the shear modulus value between 10 and 20% from loosely compacted MSW to densely compacted MSW. This agrees with our results, namely a low shear modulus between 4.6 and 5.0 MPa and low shear wave velocities between 86 and 89 m/s (from cross-hole test).

The biodegradation of the grounded MSW is characterized by the loss of mass to the medium external to the solid of waste (leachate and gas), accompanied by internal rearrangement of the particles and decrease of volume, consequently, the particle-size decrease and increase of the unit weight (Babu et al. 2014). So, it affects the material properties and, consequently,  $V_p$  and  $V_s$  measured. In this research, the  $V_p$  and  $V_s$  were obtained for MSW with 6 years of grounding, for experimental cell, and 3 years of grounding, for lysimeter. The age of grounding for this study is lower than the ages of grounding for comparative studies Abreu (2015) and Carvalho (1999), which agree with the lower velocities found here.

All the factors mentioned above, such as high content of organic material, low compaction energy, thin cover layer, apart from the climatic conditions contribute to changes in the pore fluid saturation, effective stress, pore pressure, and unit weight, which have implications on the seismic wave velocities.

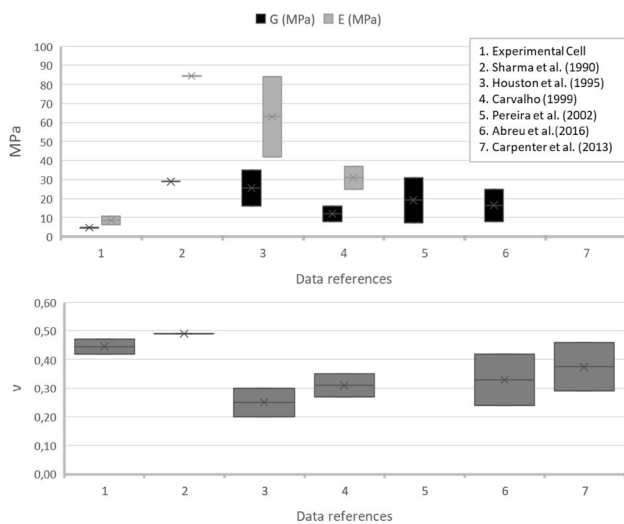


**Fig. 16** Shear and Young's modulus and Poisson ratio obtained in this research compared to other studies

The elastic properties obtained in this study and from other studies are compared in Fig. 16. The values for shear modulus ( $G$ ) and Young's modulus ( $E$ ) are lower in this study, while the range for the Poisson ratio obtained in this study is higher than the values obtained in other studies, probably because the experimental cell is only about 5 m thick and not laterally confined.

## Conclusions

Two experimental prototypes (a large in situ cell and a large-scale lysimeter) located in the City of Campinas-SP, Brazil were studied, which have some characteristics similar to those mentioned above. In this study, different seismic methods (seismic refraction tomography, multichannel analysis of surface waves, crosshole, and direct wave measurements) were combined to obtain P- and S-wave velocities. That is, the values were derived from independent tests.

The P-wave velocities obtained using SRT in the in situ experimental cell ranged between 160 and 220 m/s for the first 1.6 m depth. The P-wave velocity from the lysimeter, obtained using direct transmitted waves, ranged between 185 and 244 m/s. The P-wave obtained using crosshole tests ranged between 217 and 252 m/s. These values are lower than or within the lower bound of the velocities reported in the general literature; however, they are in accordance with the values obtained in landfills located in countries with similar socioeconomic and climatic conditions.

The average S-wave velocity for the experimental cell obtained by combining active and passive MASW is 58 m/s. The S-wave obtained using crosshole tests ranged between

86 and 89 m/s. Both the values are also in the lower range of the values reported in the literature.

These low values are characteristic of Brazilian landfills and can be attributed to their usually high content of organic material, low compaction energy, thin cover layer, apart from the climatic conditions (high pluviometry index and high temperatures). All these factors contribute to changes in the pore fluid saturation, effective stress, and pore pressure, which have implications on the seismic wave velocities.

The obtained shear modulus was between 4.6 and 5 MPa and the Young's modulus was between 6.3 and 10.9 MPa. These values are in the lower bound of results reported in general literature but are in accordance with values obtained from other Brazilian landfills.

**Acknowledgements** This work was supported by CNPq (National Council of Technological and Scientific Development, processes numbers 161961/2014-2 and 425971/2016-3) and by FAPESP (Foundation for Research Support of the State of São Paulo, processes numbers 2010/18560-4 and 2013/19778-1). The authors would also like to acknowledge the Municipality of Campinas for extending their support during the experiment and to the Institute for Technological Research of the state of Sao Paulo for their support in conducting the crosshole test.

## References

- ABNT (2004) NBR 10.004: Solid waste—Classification, Rio de Janeiro: Brazilian Association of Technical Standards (ABNT) **(in Portuguese)**
- ABNT/NB 843, N. 8., (1996) ABNT Catalog. [Online]. Available at: <https://www.abntcatalogo.com.br/norma.aspx?ID=2584>. Accessed 2019 **(in Portuguese)**
- Abreu A (2015) Geophysical research and shear strength of municipal solid waste of different ages. PhD. Thesis, School of Engineering of São Carlos, University of São Paulo **(in Portuguese)**
- Abreu A, Gandolfo O, Vilar O (2016) Characterizing a Brazilian sanitary landfill using geophysical seismic techniques. *Waste Manag* 53:116–127
- Anbazhagan P, SivakumarBabu G, LakshmiKanthan P (2016) Seismic characterization and dynamic site response of a municipal solid waste landfill in Bangalore, India. *Waste Manag Res* 34(3):205–213
- Babu G, Reddy K, Srivastava A (2014) Influence of spatially variable geotechnical properties of MSW on stability of landfill slopes. *J Hazard Toxic Radioact Waste* 18(1):27–37
- Benatti J, Paixão Filho J, Leme M, Miguel M (2013) Construction of a large-scale experimental cell to obtain hydro-geomechanical parameters of MSW of the city of Campinas, Brazil. In: Fourteenth international waste management and landfill symposium, Margherita di Pula. Proceedings. Sardinia
- Carpenter PJ, Reddy KR, ASCE F, Thompson MD (2013) Seismic imaging of a leachate-recirculation landfill: spatial changes in dynamic properties of municipal solid waste. *J Hazard Toxic Radioact Waste* 17(4):331–341
- Carvalho MF (1999) Mechanical behavior of municipal solid waste, Ph.D Thesis, University of São Paulo, São Carlos, SP, Brazil **(in Portuguese)**
- Castelli F, Maugeri M (2014) Mechanical properties of Municipal Solid Waste by SDMT. *Waste Manag* 34:256–265

- CETESB (2017) State inventory of municipal solid waste. CETESB (in Portuguese)
- Choudhury D, Savoikar P (2009) Simplified method to characterize municipal solid waste properties under seismic conditions. *Waste Manag* 29(2):924–933
- Cohen J, Stockwell JJ (1996) CWP/SU release 28, a free Seismic Software Environment For Unix Platforms. CWP-Colorado School of Mines
- Dixon N, Russell D, Jones V (2005) Engineering properties of municipal solid waste. *Geotext Geomembr* 23:205–233
- Doll W, Gamey T, Nyquist J, Mandell W, Groom D, Rohdewald S (2001) Evaluation of new geophysical tools for investigation of a landfill, Camp Roberts, California. In: 14th EEGS symposium on the application of geophysics to engineering and environmental problems
- Favery RL, Manzatto MP, Moretto RL, Almeida G, Miguel MG, Teixeira E (2016) Study of influential factors on the compaction of municipal solid waste in lysimeters. *J Solid Waste Technol Manag* 42(1):548–558
- Gaël D, Tanguy R, Nicolas M, Frédéric N (2017) Assessment of multiple geophysical techniques for the characterization of municipal waste deposit sites. *J Appl Geophys* 145:74–83
- Greenwood W, Zekkos D, Sahadewa A (2015) Spatial variation of shear wave velocity of waste materials from surface wave measurements. *J Environ Eng Geophys* 20(4):287–301
- Hoornweg D, Bhada-Tata P (2012) What a waste: a global review of solid waste management. World Bank, Washington, DC
- Houston W, Houston S, Liu J, Elsayed A, Sanders C (1995) In situ testing methods for dynamic properties. *Geotechnical Special Publication*, pp 73–82
- Kavazanjian E (2003) Evaluation of MSW properties using field measurements. In: Proceedings 17th geosynthetic research institute conference, hot topics in geosynthetics—IV
- Kavazanjian E, Matasovic N, Stokoe K, Bray J (1996) In-situ shear wave velocity of solid waste from surface wave measurements. In: Proceedings of 2nd international congress environmental geotechnics, vol 1, pp 97–104
- Konstantaki L, Ghose R, Draganov D, Diaferia G, Heimovaara T (2014) Characterization of a heterogeneous landfill using seismic and electrical resistivity data. *Geophysics* 80(1):EN13–EN25
- Konstantaki LA, Ghose R, Draganov D, Heimovaara T (2016) Wet and gassy zones in a municipal landfill from P- and S-wave velocity fields. *Geophysics* 81(6):N75–EN86
- Matasovic N, El-Sherbiny R, Kavazanjian J (2011) In-situ measurements of MSW properties. Geotechnical characterization, field measurement, and laboratory testing of municipal solid waste. American Society of Civil Engineers, New Orleans, pp 153–194
- Miguel M, Paixão Filho JL, Benatti JCB, Leme MAG, Mortatti BC, Gabrielli G, Elaiuy MLC, Pereira SY, Teixeira EN (2016) Gravimetric composition of municipal solid waste disposed in a large-scale experimental cell in Southeastern Brazil. *Int J Environ Waste Manag* 17:128–145
- Moretto RL, Siqueira Neto AC, Elis VR, Miguel MG (2017) Detection of leachate pockets in experimental cell of municipal solid waste with aid of geophysics. In: Margherita di Pula, Proceedings Sardinia 2017. CISA Publisher
- Paixao Filho JL, Miguel MG (2017) Long-term characterization of landfill leachate: impacts of the Tropical Climate on its Composition. *Am J Environ Sci* 13:116–127
- Park CB, Miller RD, Xia J, Ivanov J (2007) Multichannel analysis of surface waves (MASW)—active and passive methods. *Lead Edge* 26(1):60–64
- Sahadewa A, Zekkos D, Lobbstaal A, Woods RD (2011) Shear wave velocity of municipal solid waste in Michigan landfills. In: 14th Pan-American conference on soil mechanics and geotechnical engineering and 64th Canadian geotechnical conference on geoinnovation addressing global challenges
- Sahadewa A, Zekkos D, Woods RD, Stokoe KH (2015) Field testing method for evaluating the small-strain shear modulus and shear modulus nonlinearity of solid waste. *Geotech Test J* 38(4):427–441
- Schuster GT, Quintus-Bosz A (1993) Wavepath eikonal traveltimes inversion: theory. *Geophysics* 58(9):1314–1323
- Sharma HD, Dukes MT, Olsen DM (1990) Field measurements of dynamic moduli and Poisson's ratios of refuse and underlying soils at a landfill site. *Geotechnics of waste fills—theory and practice*. ASTM International, Philadelphia, pp 57–70
- Sheehan J, Doll WE, Mandell W (2005) An evaluation of methods and available software for seismic refraction tomography analysis. *J Environ Eng Geophys* 10:21–34
- Wongpornchai P, Phatchaiyo R, Srikoch N (2009) Seismic refraction tomography of Mae-Hia Landfill Sites, Mueang District, Chiang Mai. *World Acad Sci Eng Technol* 56:678–681
- Zalachoris G (2010) Field measurements of linear and nonlinear shear moduli of solid municipal waste using a dynamically loaded surface footing. Master of Science in Engineering. The University of Texas at Austin, Austin
- Zekkos D, Bray J, Kavazanjian E Jr, Matasovic N, Rathje E, Riemer M, Stokoe K (2006) Unit weight of municipal solid waste. *J Geotech Geoenviron Eng* 132(10):1250–1261
- Zekkos D, Bray JD, Riemer MF (2008) Shear modulus and material damping of municipal solid waste based on large-scale cyclic triaxial testing. *Can Geotech J* 45:45–58
- Zekkos D, Sahadewa A, Woods R, Stokoe K, Matasovic N (2013) In situ assessment of the nonlinear shear modulus of municipal solid waste. In: Proceedings of the 18th international conference on soil mechanics and geotechnical engineering. Paris
- Zekkos D, Sahadewa A, Woods R, Stokoe K (2014) Development of model for shear-wave velocity of municipal solid waste. *J Geotech Geoenviron Eng* 140(3):04013030

**Publisher's Note** Springer Nature remains neutral with regard to jurisdictional claims in published maps and institutional affiliations.



## Terms and Conditions

Springer Nature journal content, brought to you courtesy of Springer Nature Customer Service Center GmbH (“Springer Nature”).

Springer Nature supports a reasonable amount of sharing of research papers by authors, subscribers and authorised users (“Users”), for small-scale personal, non-commercial use provided that all copyright, trade and service marks and other proprietary notices are maintained. By accessing, sharing, receiving or otherwise using the Springer Nature journal content you agree to these terms of use (“Terms”). For these purposes, Springer Nature considers academic use (by researchers and students) to be non-commercial.

These Terms are supplementary and will apply in addition to any applicable website terms and conditions, a relevant site licence or a personal subscription. These Terms will prevail over any conflict or ambiguity with regards to the relevant terms, a site licence or a personal subscription (to the extent of the conflict or ambiguity only). For Creative Commons-licensed articles, the terms of the Creative Commons license used will apply.

We collect and use personal data to provide access to the Springer Nature journal content. We may also use these personal data internally within ResearchGate and Springer Nature and as agreed share it, in an anonymised way, for purposes of tracking, analysis and reporting. We will not otherwise disclose your personal data outside the ResearchGate or the Springer Nature group of companies unless we have your permission as detailed in the Privacy Policy.

While Users may use the Springer Nature journal content for small scale, personal non-commercial use, it is important to note that Users may not:

1. use such content for the purpose of providing other users with access on a regular or large scale basis or as a means to circumvent access control;
2. use such content where to do so would be considered a criminal or statutory offence in any jurisdiction, or gives rise to civil liability, or is otherwise unlawful;
3. falsely or misleadingly imply or suggest endorsement, approval, sponsorship, or association unless explicitly agreed to by Springer Nature in writing;
4. use bots or other automated methods to access the content or redirect messages
5. override any security feature or exclusionary protocol; or
6. share the content in order to create substitute for Springer Nature products or services or a systematic database of Springer Nature journal content.

In line with the restriction against commercial use, Springer Nature does not permit the creation of a product or service that creates revenue, royalties, rent or income from our content or its inclusion as part of a paid for service or for other commercial gain. Springer Nature journal content cannot be used for inter-library loans and librarians may not upload Springer Nature journal content on a large scale into their, or any other, institutional repository.

These terms of use are reviewed regularly and may be amended at any time. Springer Nature is not obligated to publish any information or content on this website and may remove it or features or functionality at our sole discretion, at any time with or without notice. Springer Nature may revoke this licence to you at any time and remove access to any copies of the Springer Nature journal content which have been saved.

To the fullest extent permitted by law, Springer Nature makes no warranties, representations or guarantees to Users, either express or implied with respect to the Springer nature journal content and all parties disclaim and waive any implied warranties or warranties imposed by law, including merchantability or fitness for any particular purpose.

Please note that these rights do not automatically extend to content, data or other material published by Springer Nature that may be licensed from third parties.

If you would like to use or distribute our Springer Nature journal content to a wider audience or on a regular basis or in any other manner not expressly permitted by these Terms, please contact Springer Nature at

[onlineservice@springernature.com](mailto:onlineservice@springernature.com)